

# Signature of a Dark Ultra-compact Dwarf Galaxy Transiting the Milky Way Disk

KEN UDAGAWA,<sup>1</sup> TOMOHARU OKA,<sup>1,2</sup> HIROKI YOKOZUKA,<sup>1</sup> AND TATSUYA KOTANI<sup>1</sup><sup>1</sup>*School of Fundamental Science and Technology, Graduate School of Science and Technology, Keio University, 3-14-1 Hiyoshi, Kohoku-ku, Yokohama, Kanagawa 223-8522, Japan*<sup>2</sup>*Department of Physics, Institute of Science and Technology, Keio University, 3-14-1 Hiyoshi, Kohoku-ku, Yokohama, Kanagawa 223-8522, Japan*

## ABSTRACT

We report the discovery of a vertical velocity anomaly (VVA) in the stellar component of the Galactic disk, consistent with the impact of a dark, ultra-compact dwarf galaxy (UCD)-sized object plunging into the Milky Way. The anomaly spatially coincides with a suite of gaseous disturbances—including an H I void, a molecular shell (CO 16.134–0.553), and a vertical H I filament—previously interpreted as signatures of a dark matter subhalo (DMSH) collision. Analysis of Gaia DR2 astrometry reveals a statistically significant vertical velocity dip co-located with these features, supporting a dynamical origin. The absence of a luminous source at the filament’s terminus suggests a dark or failed UCD. These results provide rare observational evidence for a low-mass DMSH, with implications for the substructure of dark matter halos and constraints on the  $\Lambda$ CDM model.

**Keywords:** Milky Way dark matter halo (1049) — Interstellar clouds (834)

## 1. INTRODUCTION

Dark matter (DM) constitutes approximately 26 % of the universe’s mass and exceeds the mass of visible baryonic matter by more than a factor of five (Planck Collaboration et al. 2020). It forms extended halos around galaxies and clusters, playing a critical role in cosmic structure formation. The leading candidate for DM is a population of cold, slow-moving, weakly interacting massive particles (WIMPs) (de Swart et al. 2017). The cold dark matter model with a cosmological constant ( $\Lambda$ CDM) has successfully explained many large-scale phenomena, such as the cosmic microwave background anisotropies, galaxy clustering, primordial element abundances, and cosmic acceleration (Riess et al. 1998; Perlmutter et al. 1999; Spergel et al. 2003; Tegmark et al. 2004).

Nonetheless, the  $\Lambda$ CDM paradigm faces notable challenges on smaller scales (Del Popolo & Le Delliou 2017). Chief among these is the “missing satellite problem,” wherein  $N$ -body simulations predict an order of magnitude more dark matter subhalos (DMSHs) around Milky Way-like galaxies ( $M_{\text{halo}} \sim 10^{12} M_{\odot}$ ) than the observed population of luminous satellite galaxies (Klypin et al.

1999; Diemand et al. 2007). While discoveries of ultra-faint dwarf galaxies have partially alleviated this discrepancy (Willman et al. 2005; Belokurov et al. 2006; Zucker et al. 2006; Sakamoto & Hasegawa 2006; Irwin et al. 2007), the population of low-mass ( $\lesssim 10^8 M_{\odot}$ ) DMSHs remains largely unconstrained due to their lack of baryonic tracers and the resolution limits of simulations.

A promising candidate for a small DMSH was identified as a broad-velocity-width molecular feature (BVF), CO 16.134–0.553, discovered during a systematic CO  $J=1-0$  survey of the Galactic disk with  $\sim 20''$  resolution (Yokozuka et al. 2021; Umemoto et al. 2017). This object spans  $\sim 5$  pc, exhibits a line width of  $\sim 30 \text{ km s}^{-1}$ , and lies at a distance of  $\sim 4$  kpc from the Sun. It shows no evident driving source, yet displays strong SiO emission indicative of dissociative shocks (Yokozuka et al. 2024), suggesting a dynamic origin. CO 16.134–0.553 marks the eastern boundary of a  $\sim 15$  pc CO shell, spatially coincident with a  $1^\circ$ -diameter H I void and a vertically oriented,  $4^\circ$ -long H I filament (Figure 1a).

The alignment of the CO shell, H I void, and filament suggests a high-velocity impact by a massive compact object, possibly a small DMSH containing some baryonic matter (Yokozuka et al. 2024). This scenario is supported by hydrodynamic simulations that reproduce the observed gaseous structures (Bekki & Chiba 2006; Tepper-García & Bland-Hawthorn 2018; Shah et al.

2019). Estimated parameters for the intruder—size 15–70 pc, velocity  $\sim 130 \text{ km s}^{-1}$ , and mass  $\sim 6 \times 10^7 M_\odot$ —place it within the expected range for low-mass DMSHs (Bovy et al. 2017; Garrison-Kimmel et al. 2017). However, these estimates are derived solely from gas morphology and simple geometry. Independent evidence, especially from stellar kinematics, is crucial to validate the DMSH impact scenario and constrain its physical properties.

## 2. DATA AND ANALYSIS

An event involving the plunge of a DMSH is expected to leave discernible traces within both the stellar population and the gaseous components of the Galactic disc. Motivated by this, we utilized astrometric data from the second data release of Gaia (Gaia DR2; Gaia Collaboration et al. 2016, 2018), which includes 1,015,747 sources within our area of interest:  $+13^\circ 0 \leq l \leq +20^\circ 0$ ,  $-8^\circ 0 \leq b \leq +5^\circ 0$ , and  $3.5 \text{ kpc} \leq D \leq 4.5 \text{ kpc}$ .

We converted the positions and proper motions of stars from equatorial (ICRS) coordinates to Galactic coordinates using the transformation procedure outlined in the Gaia Data Release Documentation provided on the ESA website<sup>3</sup>.

Subsequently, we subtracted for the systemic velocity due to Galactic rotation from the longitudinal velocities. Employing the axisymmetric, circularly rotating thin-disk model for the Milky Way Galaxy, the transverse velocity of an observed object relative to the local reference frame of stars in the solar neighborhood (the Local Standard of Rest; LSR) is given by the equation,

$$V_t = \left( \frac{\Theta}{R} - \frac{\Theta_0}{R_0} \right) R_0 \cos l - \frac{\Theta}{R} D_p. \quad (1)$$

where  $D_p = (1/\varpi) \cos b$  is the object’s distance from the sun projected onto the Galactic plane,  $\varpi$  is the parallax in mas,  $R$  is that from the Galactic center (Galactic radius),  $\Theta(R)$  is the rotation velocity at  $R$ ,  $R_0$  is the Galactic radius of the sun, and  $\Theta_0 \equiv \Theta(R_0)$ . The Galactic rotation velocity is modeled using a power-law:  $\Theta(R) = \Theta_0(R/R_0)^\alpha$ , with  $(R_0, \Theta_0, \alpha) = (8.27 \text{ kpc}, 248 \text{ km s}^{-1}, 0.05)$  (Honma et al. 2012). Since the moving direction along the Galactic rotation on the celestial sphere is parallel to the Galactic longitudinal axis, we subtracted the transverse velocity from the longitudinal velocities,

$$V_{l,c} = V_l - V_t. \quad (2)$$

In our analyses, we used  $V_{l,c}$  and  $V_b$  of stars to calculate the longitudinal and latitudinal velocity distributions.

We then averaged the rotation-corrected proper motions within each  $0^\circ 25 \times 0^\circ 25 \times 0.1 \text{ kpc}$  voxel to depict the spatial distribution of stellar velocities.

## 3. RESULTS

The analysis revealed a vertical velocity anomaly (VVA) at the root of the H I filament, as shown in Figure 1(b), with coordinates  $(l, b, D) \simeq (15^\circ 8, -0^\circ 5, 3.9\text{--}4.0 \text{ kpc})$ . We defined the spatial extent of this VVA with solid red lines in Figure 1. Within this anomaly, the average vertical (latitudinal) velocity of stars is typically  $7 \text{ km s}^{-1}$  lower than in the surrounding areas or at adjacent distances, as illustrated in Figure 2.

Although the VVA manifests as a statistically significant dip in the mean vertical velocity field, the distribution of individual stellar velocities exhibits substantial dispersion. Visualization of individual stars (Figure 3) reveals no obvious coherent concentration of stars with uniformly negative velocities. This suggests that the anomaly reflects a shift in the statistical mean of a broadly scattered velocity distribution, rather than a spatially clustered population with coherent motion.

A  $z$ -test confirmed that this deviation in average vertical velocity is statistically significant, reaching a  $6\sigma$  level. No notable variations were observed in the horizontal (longitudinal) velocity distribution, indicating that stars within the VVA predominantly exhibit negative vertical velocities. The VVA is elongated, measuring approximately 200 pc in length and 50 pc in width. Its three-dimensional location coincides with the center of the H I void at  $(l, b) \simeq (16^\circ 2, -0^\circ 05)$  and overlaps significantly with the CO shell at  $(l, b) \simeq (16^\circ 05, -0^\circ 55)$ , reinforcing the physical link between the VVA and the previously identified gaseous anomalies.

## 4. DISCUSSION

The width of the VVA, approximately 50 pc, may offer a preliminary estimate for the size of the hypothesised DMSH. The lower limit of the DMSH’s mass can be derived from the conditions for tidal stability, expressed as  $GM_{\text{DMSH}}/r_{\text{DMSH}}^2 \gtrsim GM_{\text{gal}}r_{\text{DMSH}}/R^3$ , where  $R$  is the Galactocentric distance and  $r_{\text{DMSH}}$  is the radius of the DMSH. Assuming  $M_{\text{gal}} \simeq 4 \times 10^{10} M_\odot$  (Valenti et al. 2016),  $R = 4.6 \text{ kpc}$  and  $r_{\text{DMSH}} = 25 \text{ pc}$ , the estimated lower limit for the DMSH mass is  $M_{\text{DMSH}} \gtrsim 6 \times 10^3 M_\odot$ . Another method for estimating mass is via the Hoyle-Lyttleton radius,  $r_{\text{HL}} = 2GM_{\text{DMSH}}/V_{\text{pl}}^2$ , where  $V_{\text{pl}}$  is the plunging velocity. Using  $V_{\text{pl}} = 130 \text{ km s}^{-1}$  (Yokozuka et al. 2024) and assuming  $r_{\text{HL}} \simeq r_{\text{DMSH}} = 25 \text{ pc}$ , the cal-

<sup>3</sup> [https://gea.esac.esa.int/archive/documentation/GDR2/Data\\_processing/chap\\_cu3ast/sec\\_cu3ast\\_intro/ssec\\_cu3ast\\_intro\\_transforms.html#SSS1](https://gea.esac.esa.int/archive/documentation/GDR2/Data_processing/chap_cu3ast/sec_cu3ast_intro/ssec_cu3ast_intro_transforms.html#SSS1)

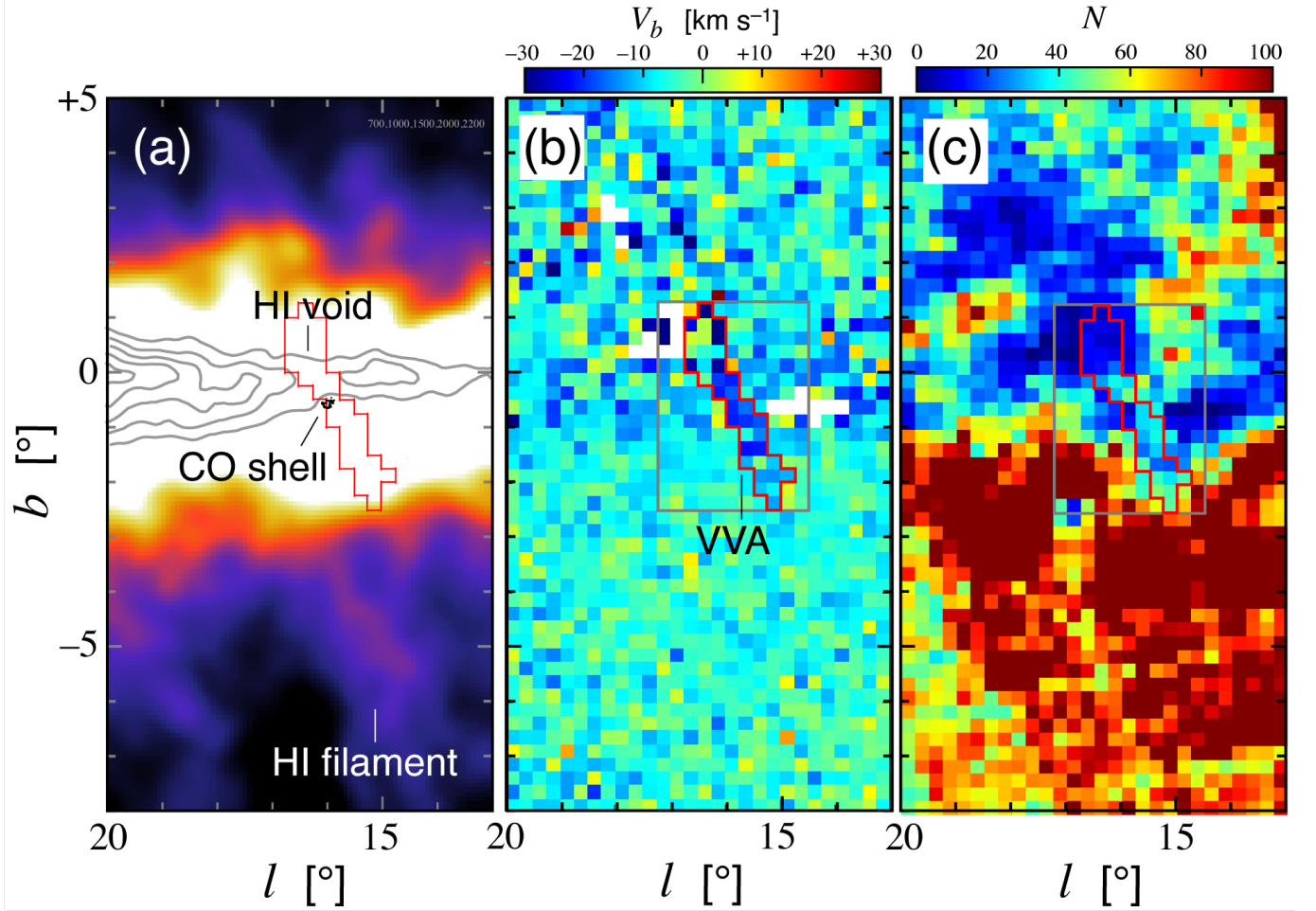


**Figure 1.** Discovery of the vertical velocity anomaly. (a) Schematic view of the anomalous features in gaseous components. The color map shows H I emission integrated over velocities between  $V_{\text{LSR}} = 40 \text{ km s}^{-1}$  and  $120 \text{ km s}^{-1}$ . Gray contours show H I emission integrated over velocities between  $V_{\text{LSR}} = 60 \text{ km s}^{-1}$  and  $100 \text{ km s}^{-1}$  at levels of 700, 1000, 1500, 2000, and 2200  $\text{K km s}^{-1}$ . (b) Distribution of the mean latitudinal (vertical) velocity of stars ( $V_b$ ) at the distance of 3.9–4.0 kpc. Pixels which contain fewer than 5 stars are shown in white. The area enclosed by solid red lines defines the vertical velocity anomaly (VVA).

culated mass of the DMSH is approximately  $M_{\text{DMSH}} \simeq 5 \times 10^7 M_{\odot}$ .

Unlike global perturbations caused by massive intruders such as the Sagittarius dwarf, which produce disk-wide warps and corrugations (e.g., [Bland-Hawthorn & Tepper-García 2021](#)), the features discussed here are highly localized. This is consistent with a lower-mass transiting object that does not significantly displace the disk center-of-mass. The absence of a significant recoil or global disk response implies that the impactor’s mass is moderate, consistent with our DMSH-scale estimate. The possible presence of large outer H I holes in galaxies (e.g., [Bosma 2017](#)) raises intriguing parallels, although such features may originate from different mechanisms including stellar feedback.

The multiwavelength context of the H I filament is shown in Figure 4. The absence of any luminous sources across radio, infrared, and X-ray bands at the tip of the H I filament suggests that the DMSH responsible for the formation of the VVA might represent a ‘dark’ or ‘failed’ dwarf galaxy, with a mass below  $10^9 M_{\odot}$ . A notable comparison is Smith’s Cloud ([Smith 1963](#)), a high-velocity H I cloud that crossed the Galactic disk approximately 70 million years ago. To have endured this passage, Smith’s Cloud is likely encapsulated within a DMSH exceeding  $10^8 M_{\odot}$  ([Nichols & Bland-Hawthorn 2009](#)). Our findings suggest a smaller analog for such dark dwarf galaxies, albeit considerably smaller than the former, with dimensions akin to those of ultra-compact dwarfs (UCDs) ([Drinkwater et al. 2000](#)), typically found in dense galaxy clusters. UCDs are char-

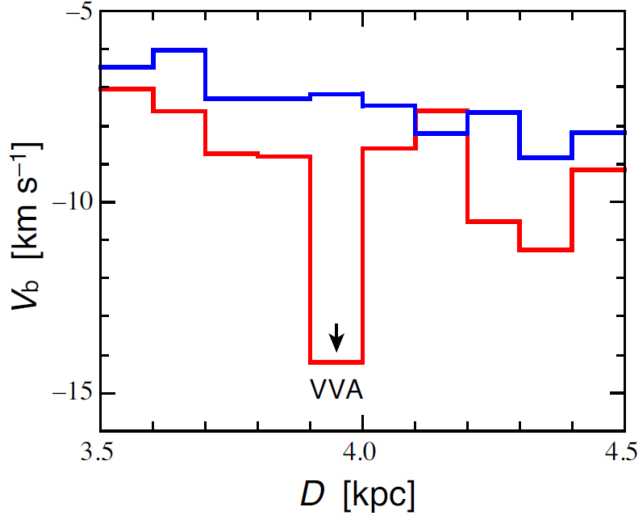


**Figure 2.** Plot of the average vertical velocity vs. distance. The red line shows the average vertical velocity of stars in the VVA, and the blue line shows that in the surrounding area (inside the gray rectangle in Figure 1(b) excluding the VVA).

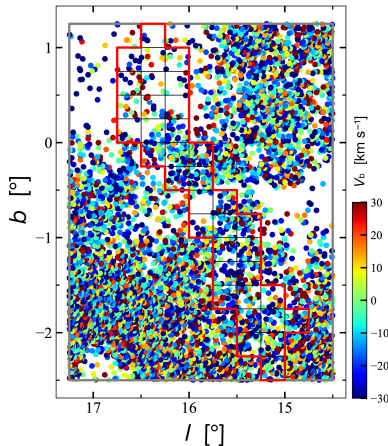


**Figure 3.** Spatial distribution of individual Gaia DR2 stars within the rectangular region indicated in Figure 1b. Each dot represents a single star and is color-coded by its vertical velocity ( $V_b$ ). The velocity scale is identical to that used in Figure 1b. A coherent group of stars with systematically negative vertical velocities is apparent, forming the vertical velocity anomaly (VVA) at the center of the frame. This visualization complements the binned median velocity map in Figure 1b by showing the unbinned stellar distribution underlying the VVA structure.

acterized by old stellar populations, half-light radii of 15–100 pc, and masses of  $10^{6.5-8} M_\odot$  (Mieske & Kroupa 2008). The possible existence of a ‘failed’ UCD—devoid of any detectable stellar component—stands in direct conflict with the prevailing formation scenario, which holds that UCDs are the stripped remnants of dwarf galaxies. If confirmed, such an object would fundamentally challenge our current understanding of compact stellar systems and their dark matter environments. Further insights into the structure of the VVA may be gained through spatial statistical analysis, such as the methods outlined by Baddeley et al. (2015).

## 5. SUMMARY

The discovery of the vertical velocity anomaly (VVA) provides compelling evidence that a low-mass dark matter subhalo (DMSH) has plunged into the Milky Way’s disk, generating a coherent set of gaseous anomalies. This finding not only supports the feasibility of using stellar kinematics to detect otherwise invisible substructures, but also motivates systematic searches for similar signatures—gaseous filaments, voids, shells, BVFs, and stellar VVAs—throughout the Galactic disk. The object inferred here, potentially a ‘failed’ ultra-compact dwarf galaxy, exemplifies a previously unrecognized class of dark halo structures. Its detection opens a new observational window onto the low-mass end of the DMSH population, offering a promising avenue to critically test the small-scale predictions of the standard  $\Lambda$ CDM cosmology and deepen our understanding of galaxy formation and dark matter.

Future surveys targeting similar kinematic and gaseous anomalies across the Galactic disk will be essential to assess the frequency and diversity of such dark subhalo events. Detailed study of the stellar populations associated with the VVA—including identification of likely member stars—may offer important clues to the nature of the impactor. Statistical modeling of the stellar distribution, such as mixture-based analysis or spatial point process methods, may further constrain the structure and origin of the velocity anomaly. These approaches will be pursued in future work.

## ACKNOWLEDGMENTS

This work made use of data from the European Space Agency (ESA) mission *Gaia* (<https://www.cosmos.esa.int/gaia>), processed by the *Gaia* Data Processing and Analysis Consortium (DPAC, <https://www.cosmos.esa.int/web/gaia/dpac/consortium>). Funding for DPAC has been provided by national institutions, in particular those participating in the *Gaia* Multilateral Agreement. We thank Editage ([www.editage.jp](http://www.editage.jp)) for English



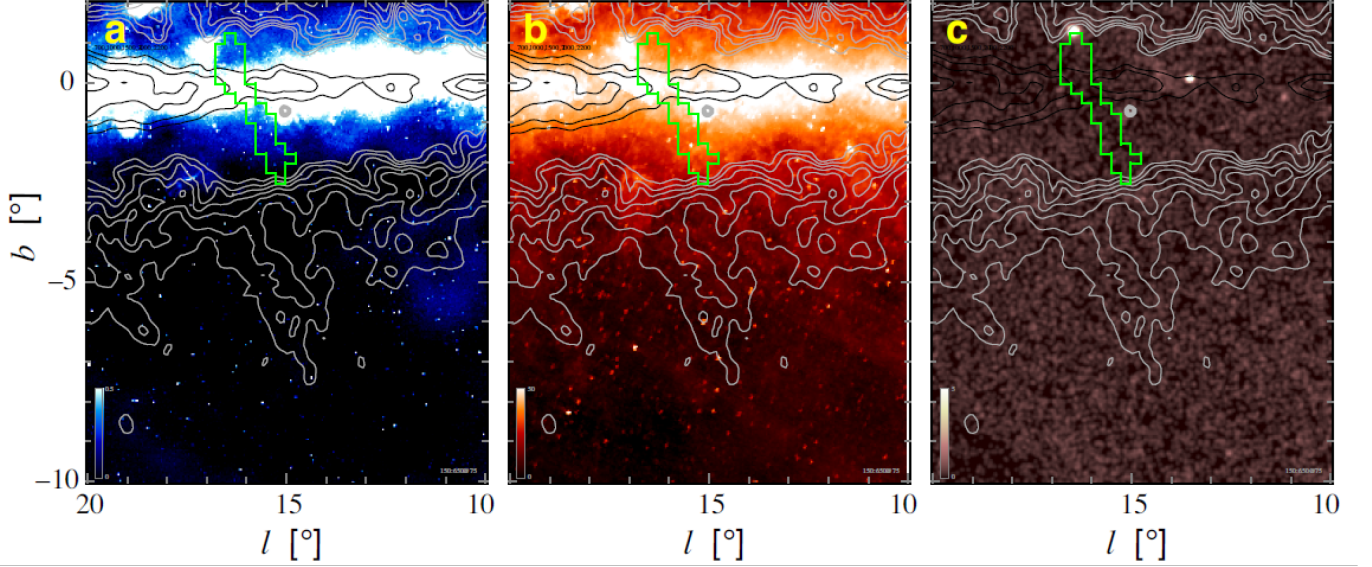


**Figure 4.** Multiwavelength views (radio, infrared, X-ray) of the region surrounding the H I filament, highlighting the absence of luminous counterparts at its tip. Colour images of (a) 170–231 MHz radio continuum, (b) IRAS 12  $\mu\text{m}$ , and (c) 0.1–2.4 keV X-ray with contours of H I integrated intensity. Light gray contours show H I emission integrated over velocities between  $V_{\text{LSR}} = 40 \text{ km s}^{-1}$  and  $120 \text{ km s}^{-1}$  at levels from  $150 \text{ K km s}^{-1}$  with  $75 \text{ K km s}^{-1}$  intervals. Dark gray contours show H I emission integrated over velocities between  $V_{\text{LSR}} = 60 \text{ km s}^{-1}$  and  $100 \text{ km s}^{-1}$  at levels of 700, 1000, 1500, 2000, and  $2200 \text{ K km s}^{-1}$ . The VVA is shown by solid green lines.

language editing. T.O. acknowledges support from JSPS KAKENHI Grant Number 20H00178.

*Software:* MATLAB

*Facilities:* Gaia, NRO 45m Telescope (FUGIN), HI4PI Survey

## REFERENCES

- Baddeley, A., Rubak, E., & Turner, R. 2015, *Spatial Point Patterns: Methodology and Applications with R* (Boca Raton, FL: CRC Press)
- Bekki, K., & Chiba, M. 2006, *ApJL*, 637, L97
- Belokurov, V., Zucker, D. B., Evans, N. W., et al. 2006, *ApJL*, 647, L111
- Bland-Hawthorn, J., & Tepper-García, T. 2021, *MNRAS*, 504, 3168
- Bosma, A. 2017, *Astrophys. Space Sci. Lib.*, 434, 209
- Bovy, J., Erkal, D., & Sanders, J. L. 2017, *MNRAS*, 466, 628
- Bullock, J. S., & Boylan-Kolchin, M. 2017, *ARA&A*, 55, 343
- de Swart, J., Bertone, G., & van Dongen, J. 2017, *NatAs*, 1, 59
- Del Popolo, A., & Le Delliou, M. 2017, *Galaxies*, 5, 17
- Diemand, J., Kuhlen, M., & Madau, P. 2007, *ApJ*, 657, 262
- Drinkwater, M. J., Jones, J. B., Gregg, M. D., et al. 2000, *PASJ*, 17, 227
- Gaia Collaboration, Prusti, T., de Bruijne, J. H. J., et al. 2016, *A&A*, 595, A1
- Gaia Collaboration, Brown, A. G. A., Vallenari, A., et al. 2018, *A&A*, 616, A1
- Garrison-Kimmel, S., Wetzel, A., Bullock, J. S., et al. 2017, *MNRAS*, 471, 1709
- Honma, M., Nagayama, T., Ando, K., et al. 2012, *PASJ*, 64, 136
- Irwin, M. J., Belokurov, V., Evans, N. W., et al. 2007, *ApJL*, 656, L13
- Klypin, A. A., Kravtsov, A. V., Valenzuela, O., & Prada, F. 1999, *ApJ*, 522, 82
- Mieske, S., & Kroupa, P. 2008, *ApJ*, 677, 276
- Nichols, M., & Bland-Hawthorn, J. 2009, *ApJ*, 707, 1642
- Perlmutter, S., Aldering, G., Goldhaber, G., et al. 1999, *ApJ*, 517, 565
- Planck Collaboration, Aghanim, N., Akrami, Y., et al. 2020, *A&A*, 641, A6
- Riess, A. G., Filippenko, A. V., Challis, P., et al. 1998, *AJ*, 116, 1009

- Sakamoto, T., & Hasegawa, T. 2006, *ApJL*, 653, L29
- Shah, M., Bekki, K., Vinsen, K., & Foster, S. 2019, *MNRAS*, 482, 4188
- Smith, G. P. 1963, *Bull. Astron. Inst. Neth.*, 17, 203
- Spergel, D. N., Verde, L., Peiris, H. V., et al. 2003, *ApJS*, 148, 175
- Tegmark, M., Strauss, M. A., Blanton, M. R., et al. 2004, *PhRvD*, 69, 103501
- Tepper-García, T., & Bland-Hawthorn, J. 2018, *MNRAS*, 473, 5514
- Umemoto, T., Minamidani, T., Kuno, N., et al. 2017, *PASJ*, 69, 78
- Valenti, E., Zoccali, M., Gonzalez, O. A., et al. 2016, *A&A*, 587, L6
- Willman, B., Dalcanton, J. J., Martinez-Delgado, D., et al. 2005, *ApJL*, 626, L85
- Yokozuka, H., Oka, T., Takekawa, S., Iwata, Y., & Tsujimoto, S. 2021, *ApJ*, 908, 246
- Yokozuka, H., Oka, T., Tsujimoto, S., Iwata, Y., & Kaneko, M. 2024, *ApJ*, 964, 52
- Zucker, D. B., Belokurov, V., Evans, N. W., et al. 2006, *ApJL*, 643, L103